



Analytical effective elastic properties of particulate composites with soft interfaces around anisotropic particles



Wenxiang Xu ^{a, b, c,*}, Huaifa Ma ^b, Shunying Ji ^c, Huisu Chen ^{d, **}

^a Institute of Soft Matter Mechanics, College of Mechanics and Materials, Hohai University, Nanjing 211100, PR China

^b State Key Laboratory of Simulation and Regulation of Water Cycle in River Basin, China Institute of Water Resources and Hydropower Research, Beijing 100048, PR China

^c State Key Laboratory of Structural Analysis for Industrial Equipment, Dalian University of Technology, Dalian 116024, PR China

^d Jiangsu Key Laboratory of Construction Materials, School of Materials Science and Engineering, Southeast University, Nanjing 211189, PR China

ARTICLE INFO

Article history:

Received 11 January 2016

Received in revised form

25 March 2016

Accepted 10 April 2016

Available online 11 April 2016

Keywords:

Particle-reinforced composites

Interface

Elastic properties

Multiscale modeling

ABSTRACT

Understanding the effects of interfacial properties on effective elastic properties is of great importance in materials science and engineering. In this work, we propose a theoretical framework to predict the effective moduli of three-phase heterogeneous particulate composites containing spheroidal particles, soft interfaces, and a homogeneous matrix. We first derive the effective moduli of two-phase representative volume elements (RVEs) with matrix and spheroidal inclusions using the variational principle. Subsequently, an analytical model considering the volume fraction of soft interfaces around spheroidal particles is presented. The effective moduli of such three-phase particulate composites are eventually derived by the generalized self-consistent scheme. These theoretical schemes are compared with experimental studies, numerical simulations, and theoretical approximations reported in the literature to verify their validity. We further investigate the dependence of the effective elastic modulus on the interfacial properties and the geometric characteristics of anisotropic particles based on the proposed theoretical framework. Results show that the interfacial volume fraction and the effective elastic modulus of particulate composites are strongly dependent on the aspect ratio, geometric size factor, volume fraction, and particle size distribution of ellipsoidal particles.

© 2016 Elsevier Ltd. All rights reserved.

1. Introduction

Interfaces interacted by anisotropic particles are crucial components in a variety of particulate materials like polymer, colloidal, ceramic, and cementitious composites [1–4]. Understanding the effects of interfacial characteristics on effective elastic properties as average features by homogenization that well reflect the macroscopic mechanical responses of particulate composites, is a problem of great interest in materials research & development [3–7]. Specifically, the estimation of effective moduli of particulate composites is of prime importance to better capture the behaviors of composites and to evaluate the success of their design. In the present work, we focus on spheroids as shape-anisotropic particles over a broad range of aspect ratios with widespread applications in

specific materials [1,4–6].

It has been experimentally observed by several imaging equipment that interfaces as a weak link have a complex network that adjacent interfaces possess an overlap potential in some particulate composites, such as cementitious, ceramic, and colloidal composites, where the formation of interfaces normally attributes to the packing of discrete grains against aggregate or wall surfaces, namely, the so-called “wall” effect [8–10]. This also gives rise to the physical natures of a relative high porosity and low rigidity for interfaces around aggregates. As such, interfaces are usually viewed as a compliant interphase (i.e., soft interfaces) between inclusions and matrix [2,4,7–9], as well as particulate composites as a three-phase composite structure consist of inclusions, soft interfaces, and matrix.

Over the past decades, the researches for effective elastic properties of three-phase particulate composites have attracted much attention, especially for the three-phase composites containing interfaces. The pioneering work was from Christensen and Lo [11] that applied the generalized self-consistent scheme [12] to

* Corresponding author. Institute of Soft Matter Mechanics, College of Mechanics and Materials, Hohai University, Nanjing 211100, PR China.

** Corresponding author.

E-mail addresses: wxxfat@gmail.com (W. Xu), chenhs@seu.edu.cn (H. Chen).

study the effective shear modulus of three-phase composites with spherical inclusions. Thereafter, many seminal empirical and theoretical formulae have been proposed to predict effective moduli of three-phase composites, such as bounds models [13,14], Mori-Tanaka scheme [15], differential effective medium approximation [16], generalized self-consistent scheme [12,17], and series expansions [18], and other effective medium methods. Fu et al. [19] and Wang and Pan [20] have well summarized the existing studies in this area, interested readers may refer to the two reviews. Also, three kinds of interfacial model are often used to simulate the properties of interfaces in those effective medium methods: the linear-spring model, interface stress model, and interphase model [7]. The first two models assume interfaces occupying a zero volume in composites that is essentially a two-phase composite structure, whereas, the third one is a three-phase model, composed of inclusions, interphase, and matrix, similar to the present case. From view of the abovementioned micromechanics schemes, the estimation of effective moduli of composites requires knowledge of the volume fraction and elastic properties of individual phases [11–20]. Therefore, as an important microstructural characteristic, the volume fraction of interphase should be considered to investigate the effective elastic properties of three-phase composites. As demonstrated by Torquato [5], the more microstructural characteristics of composite media are explored, the more accurate their effective properties can be estimated. It is worth mentioning that Garboczi and Bentz [21] presented a theoretical approximation for the volume fraction of soft interfaces around spherical particles, and the theoretical model was further employed to predict the effective conductivity of cementitious composites. Although such the outstanding contribution may provide guidance for the effective elastic properties of particulate composites, isotropic spheres cannot reflect the anisotropy nature of particles in particulate composites. Also, the volume fraction of soft interfaces around anisotropic particles has received relatively little attention in terms of theoretical modeling until fairly recently [4,22–24]. Moreover, it is quite challenging to evaluate the effect of such the interfacial property on the elastic moduli of particulate composites with anisotropic ellipsoidal particles and soft interfaces.

In the present study, heterogeneous particulate composites consist of a homogeneous matrix, anisotropic spheroidal particles, and soft interfaces. Perfect bonding conditions are assumed to prevail at both the particle/interface and the interface/matrix. We attempt to develop a theoretical framework to predict the effective moduli of particulate composites, in order to provide an efficient tool for their design. We first demonstrate a theoretical scheme for predicting the effective moduli of two-phase composites with spheroidal inclusions. We give an analytical approximation for the volume fraction of soft interfaces around ellipsoidal particles. Subsequently, by the generalized self-consistent scheme, the prediction of the effective moduli of heterogeneous three-phase particulate composites is explicitly presented in details. The rest of this article is organized as follows. Section 2 demonstrates the effective moduli of two-phase composites. Section 3 presents the volume fraction of soft interfaces around ellipsoidal particles. In Section 4, the effective moduli of three-phase composites are proposed. Subsequently, the theoretical results are given and discussed in Section 5. Finally, this article is completed with some concluding remarks in Section 6.

2. Effective moduli of two-phase composites

As mentioned above, several attempts have been made for theoretically investigating the effective moduli of particulate composites. It is worth mentioning that Wills and co-workers [25,26] applied a generalized variational principle to propose

estimates of the Hashin-Shtrikman (HS) type for composites with ellipsoidal inclusions and considering their spatial distribution configurations. In that approximation, the RVE of an ergodic M -phase heterogeneous composite consists of $M-1$ types of ellipsoidal inclusions, distributed in a homogeneous matrix (denoted as phase 1, with modulus tensor \mathbf{E}_1). It is assumed that there are m_r inclusions of type r ($r = 2, 3, \dots, M$), with modulus tensor \mathbf{E}_r . The basic derivation of effective moduli is illustrated in [Supplementary Information \(see S1\)](#). In that framework, a suitable choice for the comparison material is the matrix material itself, i.e., $\mathbf{E}_0 = \mathbf{E}_1$, so that the polarization field vanishes exactly in the matrix phase and the microstructural tensor $\langle \mathbf{A}_{rs} \rangle$ for this kind of RVE can be expressed by

$$\langle \mathbf{A}_{rs} \rangle = f_r(\delta_{rs}\mathbf{L}_{ir} - f_s\mathbf{L}_{drs}), (r, s = 2, \dots, M) \quad (1)$$

where f_r is the volume fraction of inclusions of type r , tensors \mathbf{L}_{ir} and \mathbf{L}_{drs} are associated with the inclusion and distribution shape tensors \mathbf{Z}_{ir} and \mathbf{Z}_{drs} , respectively. \mathbf{L}_{ir} is defined as [27]

$$\mathbf{L}_{ir} = \frac{1}{4\pi|\mathbf{Z}_{ir}|} \int_{|\xi|=1} \mathbf{C}_0(\xi) |\mathbf{Z}_{ir}^{-1} \cdot \xi|^{-3} dS(\xi) \quad (2)$$

where the integration is operated over the unit sphere $|\xi| = 1$, $C_{0mn} = 1/E_{1mn}\xi_m\xi_n$, and ξ_m is one of components of the unit vector. Similarly, \mathbf{L}_{drs} can also be expressed by an analogous to Eq. (2) with \mathbf{Z}_{ir} replaced by \mathbf{Z}_{drs} . The inverses of the eigenvalues of \mathbf{Z}_{ir} and \mathbf{Z}_{drs} are the semi-axes of the ellipsoidal inclusion and the distribution ellipsoid, respectively. If the distribution of inclusions is the same, i.e., $\mathbf{L}_{drs} = \mathbf{L}_d$, \mathbf{L}_d and \mathbf{L}_{ir} can be characterized by Eshelby tensors \mathbf{H}_V and \mathbf{H}_r , which represent the geometric factor tensors of the distribution ellipsoid and the ellipsoidal inclusions of type r correspondingly. Herein, we follow the works of Torquato [5] and Duan et al. [27], where the 2 s-order tensors are displayed by the elliptical integrals

$$\mathbf{H}_j = \frac{a_{1j}a_{2j}a_{3j}}{4\pi} \int_{|\xi|=1} \frac{\mathbf{C}_0(\xi) \cdot \mathbf{E}_1}{r^3} dS(\xi), (j = r, V) \quad (3)$$

with

$$r^2 = a_{1j}^2\xi_1^2 + a_{2j}^2\xi_2^2 + a_{3j}^2\xi_3^2$$

where a_{1j} , a_{2j} , and a_{3j} are the semi-axes of the j th ellipsoidal inclusion. For a spheroidal inclusion, its symmetry axis is aligned along the Z-axis, namely, $a_{1j} = a_{2j} = a$, and $a_{3j} = b$. \mathbf{H}_V and \mathbf{H}_r have exactly diagonal eigenvalues, that is

$$\mathbf{H}_j = \begin{bmatrix} H_j & 0 & 0 \\ 0 & H_j & 0 \\ 0 & 0 & 1 - 2H_j \end{bmatrix}, (j = r, V) \quad (4)$$

with

$$H_j = \frac{1}{2} \left\{ 1 + \frac{1}{\kappa^2 - 1} \left[1 - \frac{\kappa}{2\sqrt{\kappa^2 - 1}} \ln \left(\frac{\kappa + \sqrt{\kappa^2 - 1}}{\kappa - \sqrt{\kappa^2 - 1}} \right) \right] \right\}, \kappa \geq 1 \quad (5a)$$

$$H_j = \frac{1}{2} \left\{ 1 + \frac{1}{\kappa^2 - 1} \left[1 - \frac{\kappa}{\sqrt{1 - \kappa^2}} \arctan \left(\frac{\sqrt{1 - \kappa^2}}{\kappa} \right) \right] \right\}, \kappa \leq 1 \quad (5b)$$

where κ is the aspect ratio of spheroid defined as $\kappa = b/a$. If $\kappa > 1$, the spheroid is prolate; if $\kappa < 1$, the spheroid is oblate. For some special cases of the spheroid, for instance, a sphere ($\kappa = 1$), $H_j = 1/3$; a needle-shaped particle (e.g., fiber, $\kappa = \infty$), $H_j = 1/2$; a disk-shaped particle (e.g., platelet, $\kappa = 0$), $H_j = 0$. Thus, according to Eqs. (2) and (3), \mathbf{L}_{ir} and \mathbf{L}_d can be explicitly expressed by

$$\mathbf{L}_{ir} = \mathbf{H}_r \cdot \mathbf{E}_1^{-1}, \mathbf{L}_d = \mathbf{H}_V \cdot \mathbf{E}_1^{-1} \quad (6)$$

Combination of Eq. (17) in S1 and Eqs. (1) and (6), the effective moduli tensor $\bar{\mathbf{E}}$ of an ergodic M -phase heterogeneous composite consisting of $M-1$ types of ellipsoidal inclusions, distributed with ellipsoidal symmetry in matrix can be represented as

$$\bar{\mathbf{E}} = \mathbf{E}_1 + \mathbf{E}_1 \cdot \left[\left(\sum_{r=2}^M \mathbf{T}_r \right)^{-1} - \mathbf{H}_V \right]^{-1} \quad (7)$$

where

$$\mathbf{T}_r = f_r \left[(\mathbf{E}_r - \mathbf{E}_1)^{-1} \cdot \mathbf{E}_1 + \mathbf{H}_r \right]^{-1} \quad (8)$$

In the following, we consider the microstructure of a two-phase particulate composite that anisotropic spheroidal inclusions of the same type (e.g., possessing a constant aspect ratio) are randomly distributed in a homogeneous matrix with an elastic modulus E_1 , shear modulus G_1 , bulk modulus K_1 , Poisson ratio ν_1 , and volume fraction f_1 , as shown in Fig. S1. The spheroidal inclusions have an elastic modulus E_2 , shear modulus G_2 , bulk modulus K_2 , Poisson ratio ν_2 , and volume fraction f_2 . These elastic properties are related as follows

$$G_i = \frac{E_i}{2(1 + \nu_i)}, K_i = \frac{E_i}{3(1 - 2\nu_i)}, (i = 1, 2) \quad (9)$$

$$\nu_i = \frac{(3K_i - 2G_i)}{2(3K_i + G_i)}, \frac{9}{E_i} = \frac{1}{K_i} + \frac{3}{G_i}, (i = 1, 2) \quad (10)$$

Without loss of generality, we here take the effective elastic modulus as elastic properties of our focus. In the current case, the RVE of randomly distributed spheroids is isotropic. The shape of the distribution spheroid should thus be spherical, namely, $H_V = 1/3$. The effective elastic modulus of two-phase RVE can be calculated by substituting $M = 2$ into Eq. (7).

$$\bar{\mathbf{E}} = E_1 + E_1 \cdot \left[(T_2)^{-1} - \frac{1}{3} \right]^{-1} \quad (11)$$

where

$$T_2 = \frac{1}{3} f_2 (E_2 - E_1) \left[\frac{2}{E_1 + H_2(E_2 - E_1)} + \frac{1}{E_1 + (1 - 2H_2)(E_2 - E_1)} \right] \quad (12)$$

3. Volume fraction of soft interfaces

In this work, the microstructure of a three-phase particulate composite is composed as the well-known hard core-soft shell structured particles [28], in which the interfacial layer as a soft shell of a predefined dimension is coated on the surface of each hard spheroidal core, as shown in Fig. 1. It is worth mentioning that the construction of interfacial layers of a constant dimension can be realized by the Minkowski addition manner, the detailed

procedures of which can be found in the recent reference [24]. We adopt our preliminary work that the soft interfacial volume fraction around polydisperse spheroidal particles is obtained by an approximate theoretical scheme [22], as depicted the following formula. The detailed derivation is presented in Supplementary Information (see S3).

$$V_{si} = (1 - V_p) \left\{ 1 - \exp \left[- \frac{6V_p}{\langle D_{eq}^3 \rangle} (e^{(s)}t + d^{(s)}t^2 + g^{(s)}t^3) \right] \right\} \quad (13)$$

where V_{si} and V_p are the volume fractions of soft interfaces and hard particles, respectively. D_{eq} is an equivalent diameter as the size of anisotropic particles defined as the diameter of a sphere having the same volume as the anisotropic particle. $\langle \rangle$ indicates a number-averaged treatment in polydisperse spheroidal particle systems different from that depicted in S1. t is the interfacial thickness. $e^{(s)}$, $d^{(s)}$, and $g^{(s)}$ are the parameters, the formulae for which are expressed as Eqs. (30)–(32) in S3, respectively. For monodisperse three-phase RVEs, we prescribe a geometric size factor λ to reflect the coupling effect between the interfacial dimension and the particle size, namely, $\lambda = t/D_{eq}$. Thus, the interfacial volume fraction in monodisperse three-phase RVEs is expressed as

$$V_{si} = (1 - V_p) \left(1 - \exp \left\{ - \frac{6V_p}{(1 - V_p)} \left[\frac{1}{n(\kappa)} \lambda \right. \right. \right. \\ \left. \left. \left. + \left(2 + \frac{3V_p}{n^2(\kappa)(1 - V_p)} \right) \lambda^2 + \frac{4}{3} \left(1 + \frac{3V_p}{n(\kappa)(1 - V_p)} \right. \right. \right. \right. \\ \left. \left. \left. \left. + \frac{mV_p^2}{n^3(\kappa)(1 - V_p)^2} \right) \lambda^3 \right] \right\} \right) \quad (14)$$

where $n(\kappa)$ is the sphericity of a spheroidal particle defined as the ratio of the surface area between a sphere and a spheroid with the same volume (see Eq. (29) in S3). m is a parameter equivalent to 0, 2 or 3, the explanation of which is illustrated in S3. From the above formula, it can be found that the interfacial volume fraction in monodisperse RVEs predominantly relies on the geometric size factor λ and the geometric shape of anisotropic spheroidal particles, in addition to the volume fraction of particles. That suggests the constant λ with different t and D_{eq} possessing the uniform V_{si} .

4. Effective moduli of three-phase composites

We here employ a three-layer composite spheroid assemblage model representing the three-phase RVE to capture the effective elastic modulus of particulate composites, as shown in Fig. 2. The blue spheroidal inclusion, gray shell, and yellow shell in Fig. 2 represent the particle phase, interface phase, and matrix, respectively. It is supposed that the three spheroidal shells possess concentric and the elastic modulus of each phase in all directions is the same, at least, as an average. Our strategy starts that the three-phase composite structure is divided into two two-phase cells: the first one consists of the particle phase and interface phase; the second one is viewed as matrix and a composite particle phase composed of hard particle and its adjacent interface, as shown in Fig. 2. Each two-phase cell as a basic object of study is investigated to derive the effective elastic modulus of particulate composites. We consider the first two-phase cell, in which hard particles and interfaces are regarded as inclusions and a matrix, respectively. Based on the results illustrated in Section 2, the effective elastic modulus of the first two-phase composite cell can be given by

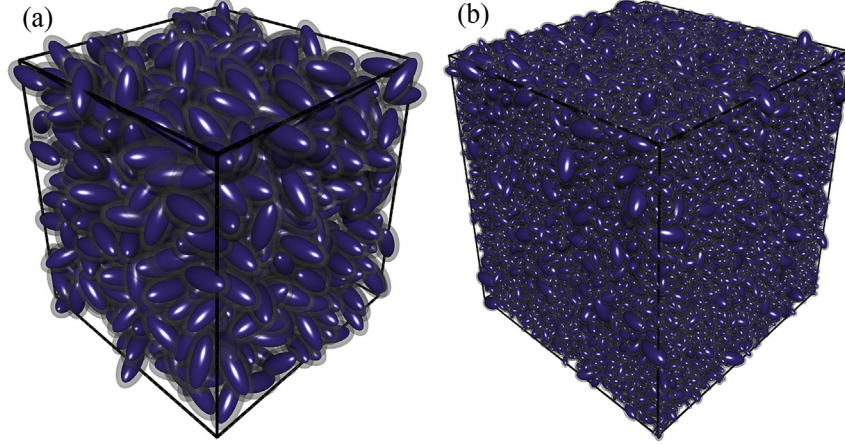


Fig. 1. Visualizations of three-phase RVEs composed of anisotropic particles (i.e., blue spheroids), soft interfaces (i.e., transparent spheroidal shells), and a homogeneous matrix. The interfacial dimension of $t = 2.0$ and other parameters are in agreement with that demonstrated in Fig. S1. (For interpretation of the references to colour in this figure legend, the reader is referred to the web version of this article.)

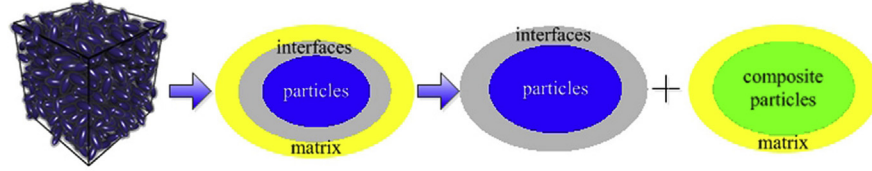


Fig. 2. Schematic view of the three-layer composite spheroid assemblage model, which is divided into two two-phase cells.

$$\bar{E}^{(1)} = E_i + E_i \cdot \left[\left(T_2^{(1)} \right)^{-1} - \frac{1}{3} \right]^{-1} \quad (15)$$

with

$$T_2^{(1)} = \frac{1}{3} f_2^{(1)} (E_p - E_i) \left[\frac{2}{E_i + H_2^{(1)} (E_p - E_i)} + \frac{1}{E_i + (1 - 2H_2^{(1)}) (E_p - E_i)} \right] \quad (16)$$

where $\bar{E}^{(1)}$ is the effective elastic modulus of the first two-phase cell, which is essentially equivalent to the elastic modulus of the composite particle phase mentioned in the second two-phase cell. E_p and E_i are the elastic moduli of hard particles and interfaces (i.e., $E_2 = E_p$, $E_1 = E_i$), respectively. $H_2^{(1)}$ is the geometric factor of hard particles with a constant aspect ratio of κ , as expressed by Eq. (5). $f_2^{(1)}$ is the volume fraction of inclusions in the first one, which should equal to the volume fraction of hard particles occupying to the whole cell with particles and interfaces, i.e., $f_2^{(1)} = V_p/(V_p + V_{si})$.

We further investigate the second one, in which the composite particles are viewed as inclusions (see Fig. 2). In doing so, $E_2 = \bar{E}^{(1)}$, $E_1 = E_m$, where E_m is the elastic modulus of matrix in particulate composites. Similarly, in terms of Eqs. (11), (12), (15) and (16), the effective elastic modulus of the second one, namely, the effective elastic modulus of the three-phase composite RVE, is presented as:

$$E_e = E_m + E_m \cdot \left[\left(T_2^{(2)} \right)^{-1} - \frac{1}{3} \right]^{-1} \quad (17)$$

with

$$T_2^{(2)} = \frac{1}{3} f_2^{(2)} (\bar{E}^{(1)} - E_m) \left[\frac{2}{E_m + H_2^{(2)} (\bar{E}^{(1)} - E_m)} + \frac{1}{E_m + (1 - 2H_2^{(2)}) (\bar{E}^{(1)} - E_m)} \right] \quad (18)$$

where E_e is the effective elastic modulus of particulate composites of three-phase structure. $f_2^{(2)}$ is the volume fraction of the composite particle phase in the second cell that is actually the region of hard particles and interfaces occupying to particulate composites, i.e., $f_2^{(2)} = V_p + V_{si}$. $H_2^{(2)}$ is the geometrical factor of composite particles with the aspect ratio κ_c . Note that the aspect ratio of composite particles is not the aspect ratio of hard particles, $\kappa_c \neq \kappa$, since the three semi-axes of a composite spheroidal particle should be $a + t$, $a + t$, and $b + t$ (a , a , and b are the semi-axes of the corresponding hard particle, see Section 2), respectively. In terms of the definitions of equivalent diameter and geometric size factor mentioned in Section 3, the aspect ratio κ_c of composite spheroidal particles can be given by

$$\kappa_c = \frac{b + t}{a + t} = \frac{0.5D_{eq}\kappa^{2/3} + t}{0.5D_{eq}\kappa^{-1/3} + t} = \frac{0.5\kappa^{2/3} + \lambda}{0.5\kappa^{-1/3} + \lambda} \quad (19)$$

It can be seen from the above formula that the aspect ratio of composite spheroidal particles is not only dependent on the aspect ratio of hard particles, but also the geometric size factor. Interestingly, when the interfacial dimension is much smaller than the particle size, namely, $\lambda \rightarrow 0$, the present composite spheroid assemblage is just reduced as isomorphic ellipsoidal shells, which is distinctively different from those composite spheroid models reported in the previous researches [4,25–27].

We also consider several special issues of ellipsoidal particles mentioned in Section 2, such as spheres ($\kappa = 1$, $H_2 = 1/3$), fibers ($\kappa = \infty$, $H_2 = 1/2$), and platelets ($\kappa = 0$, $H_2 = 0$). If anisotropic ellipsoids degenerate to spheres, the effective elastic modulus of particulate composites is reduced to

$$E_e = E_m + E_m \cdot \frac{3f_2^{(2)}(\bar{E}^{(1)} - E_m)}{3E_m + (1 - f_2^{(2)})\bar{E}^{(1)} - E_m} \quad (20)$$

with

$$\bar{E}^{(1)} = E_i + E_i \cdot \frac{3f_2^{(1)}(E_p - E_i)}{3E_i + (1 - f_2^{(1)})(E_p - E_i)} \quad (21)$$

Moreover, if the interfacial dimension equals to zero, namely, $V_{si} = 0$ and $f_2^{(1)} = 1$, so that $\bar{E}^{(1)} = E_p$, the present result reduces to the well-known Hashin-Shtrikman (HS) lower bound. Similarly, we can obtain the effective elastic moduli of fibrous composites and platelet composites by submitting of their H_2 into Eqs. (16) and (18).

5. Results and discussion

We test the theoretical frameworks proposed above. First of all, we compare the theoretical scheme for the effective elastic modulus of two-phase composites presented in Section 2 with those theoretical approximations such as HS bounds [13], Maxwell–Garnett/Wagner (MG/MW) models [29], and self-consistent scheme [12], and with experimental data from both uniaxial tension and compression of cementitious composites [30], as shown in Fig. 3. The inclusions are considered as spherical particles in agreement with that displayed in those theoretical approximations. As illustrated aforementioned, for two-phase particulate composites composed of spherical particles, the present theoretical scheme reduces to the HS lower bound and MG/MW models, as well as the results are lower than that from self-consistent scheme, as shown in Fig. 3. Fig. 3 shows that the tendency of the present scheme satisfies with the experimental results, though the theoretical

prediction is slightly higher than the experimental data outside the HS bounds. This implies that the interfacial effect needs to be considered in the theoretical prediction of elastic properties of particulate materials. In addition, we further compare the present theoretical framework and the experimental results of mortar reported by Yang [31], as shown in Table 1. We find that the present two-phase theoretical framework overestimates the elastic modulus of mortar, compared with the experimental data. It is further validated that the interfacial effect significantly affects the overall elastic properties of particulate composites, since experimental and numerical studies have confirmed that relatively porous interfacial zones with lower stiffness (with respect to matrix) exist around hard particles in some specific composites like cementitious, ceramic, and glass materials [8–10,29–31]. Therefore, it is necessary to draw into the interfacial phase in the theoretical prediction.

We then compare the theoretical results of interfacial volume fraction from the theoretical scheme introduced in Section 3 with that of numerical results in monodisperse three-phase RVEs. The numerical estimation of interfacial volume fraction is based on a Monte Carlo random point sampling algorithm, which has been elaborated in our preliminary works [22,23]. As expected, Fig. 4 displays that the theoretical results are in good agreement with the numerical results for different aspect ratios κ and geometric size factors λ . It indicates that the stability of the proposed theoretical model for the interfacial volume fraction is favorable. From Fig. 4, we find that, at a constant λ , the interfacial volume fraction V_{si} dramatically decreases with increasing κ of oblate spheroids, and gradually increases with increasing κ of prolate spheroids. Specifically, when κ equals to unity, meaning that spheroids degenerate to spheres, V_{si} has the smallest value. It suggests that anisotropic particles give rise to an increment of the interfacial volume fraction compared to isotropic spheres. The conclusion is similar with that for polydisperse three-phase RVEs [4]. Actually, such conclusion validates a significant issue that the packing density of ellipsoids sharply increases as anisotropic particles deviate slightly from perfect spheres, studied by computer simulations in the literature [32–34]. Indeed, the packing of hard particles is denser; the overlap potential of interfaces is more prominent, so that the interfacial volume fraction expectedly increases. Interestingly, the interfacial volume fraction increases with the increase of geometric size factor λ . In other words, the interfacial volume fraction intensively depends on the coupling of the interfacial dimension and the equivalent diameter, rather than the single factor.

Fig. 5 presents a comparison of the effective elastic moduli of three-phase composites containing interface phase computed by the theoretical framework demonstrated in Section 4 with experimental data of granular materials including grains of various types like glass, gravel, limestone, and lead [35]. It can be seen that the theoretical results are consistent with experimental data of different grains. We further apply the theoretical framework to predict the overall elastic moduli of three-phase particulate composites with two interfacial dimensions of $t = 20 \mu\text{m}$ and $40 \mu\text{m}$, and compare with experimental data reported by Yang [31] and with the two-phase theoretical scheme without interface phase, as shown in Fig. 6. As expected, we can see that the predicted results of three-phase theoretical framework are closer to the experimental data, compared to that of the two-phase theoretical scheme. Especially for the higher particle volume fraction, the difference between the three-phase theoretical framework and the two-phase theoretical scheme is more prominent with respect to the experimental data. It shows that the interfacial effect becomes more significant as the particle volume fraction increases. On the other hand, in the Supplementary Information (S4), Fig. S3 displays the effect of the selection of elastic modulus of interfaces E_i on the

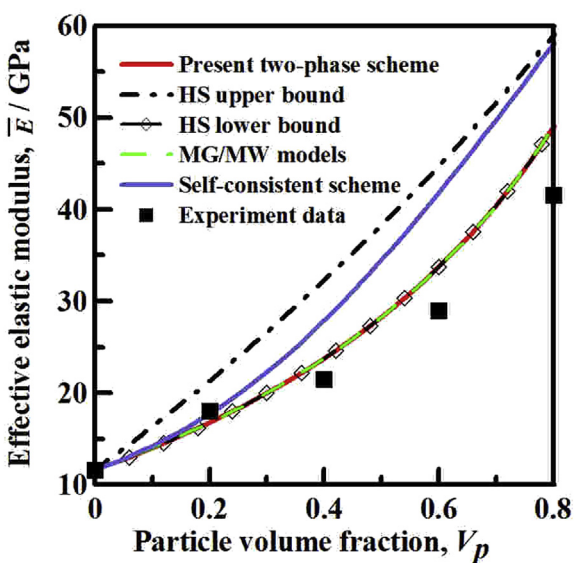


Fig. 3. Comparisons of the proposed theoretical scheme for the effective elastic modulus of two-phase composites with the existing theoretical approximations, and with experimental data reported by Stock et al. [30]. Theoretical parameters follow the experimental conditions, such as $E_m = 11.6 \text{ GPa}$ and $E_p = 75.5 \text{ GPa}$.

Table 1

Comparisons of experimental data and calculated results of elastic modulus from the present two-phase theoretical framework (theoretical parameters follow Yang's experiment that $E_m = 20.76$ GPa and $E_p = 80$ GPa [31]).

V_p	Experimental data [31] \bar{E}^a (GPa)	Calculated results \bar{E} (GPa)	Relative error $(\bar{E}-\bar{E}^a)/\bar{E}$
0	20.760	20.760	0
0.1	22.304	23.9516	0.068
0.2	24.141	27.4881	0.121
0.3	26.350	31.4284	0.161
0.4	29.292	35.8459	0.182
0.5	32.439	40.8329	0.205

^a Average of three specimens.

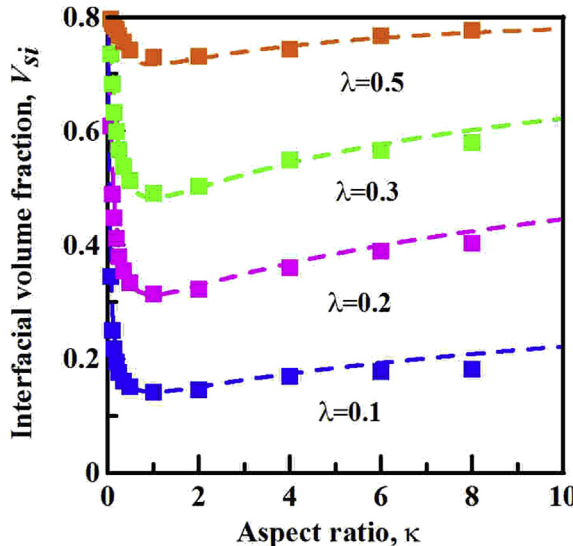


Fig. 4. Comparisons of the theoretical and numerical results of interfacial volume fraction V_{si} for various aspect ratios κ and geometric size factors λ in monodisperse three-phase RVEs. The dash lines and points (cubes) are the theoretical and numerical results of interfacial volume fraction, respectively. Without loss of generality, the particle volume fraction is here set to $V_p = 0.2$.

effective elastic modulus of particulate composites.

Fig. 7 presents the dependence of the effective elastic modulus on the aspect ratio of hard spheroidal particles in monodisperse three-phase particulate composites. From Fig. 7, we can see that, for a given V_p , the effective elastic modulus E_e increases sharply with the reduction of κ of oblate spheroids, and increases gently with the increase of κ of prolate spheroids. Interestingly, when anisotropic spheroids degenerate to isotropic spheres (i.e., $\kappa = 1.0$), E_e reaches the smallest value. This means the anisotropy of particles giving rise to an increment of the overall elastic modulus of particulate materials with a constant volume fraction of particles. Therefore, in the process of the design of particulate composites, it should be required for the consideration of the influence of geometric shape of anisotropic particles. Contrasting to Fig. 4, we are surprised to find that the influence of aspect ratio of particles on the effective elastic modulus and the interfacial volume fraction is so in agreement. It reveals that, as a critical interfacial property, the interfacial volume fraction is intimately related to the overall elastic properties of particulate composites.

Fig. 8 illustrates the impact of geometric size factor λ on the interfacial volume fraction V_{si} and the effective elastic modulus E_e for various particle volume fractions V_p . From Fig. 8(a), it can be seen that, at a constant V_p , V_{si} increases rapidly with the increase of λ , and then reaches a maximal value equivalent to $1-V_p$ as λ increases to a critical threshold. In doing so, soft interfaces overlap enough to fill up the remaining matrix. It means that the three-

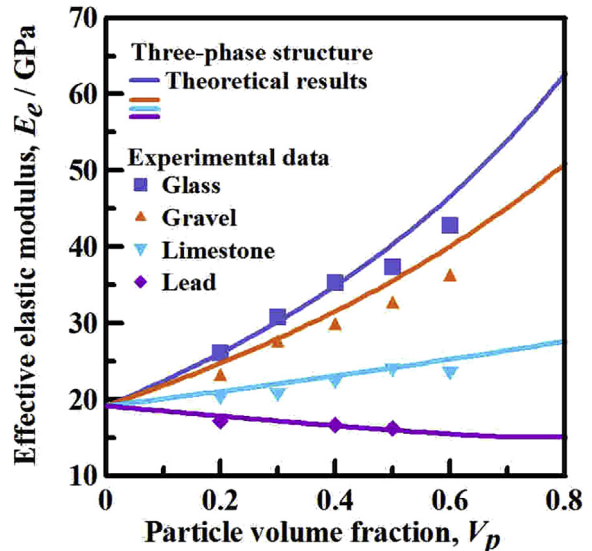


Fig. 5. Comparisons of the theoretical predicted results of effective elastic modulus of three-phase composites containing interfaces with experimental data reported by Ramesh et al. [35]. Theoretical parameters follow the experimental conditions, such as $E_m = 19.17$ GPa, $E_i = 0.5 E_m$, and $E_p = 73.1$ GPa for glass, 59.6 GPa for gravel, 30.7 GPa for limestone, and 16.6 GPa for lead. The geometric size factor and average aspect ratio of ellipsoidal particles are set to 0.01 and 2.021 from employing the unified Fourier morphological analysis reported by Wang et al. [36].

phase composite reduces to a two-phase structure composed of hard particles and interfaces, with respect to the threshold state. At this moment, the elastic modulus of $\bar{E}^{(1)}$ just represents the overall elastic modulus of particulate composites, as depicted in Eqs. (15) and (16), where $\bar{E}^{(1)}$ is only controlled by E_i and the physical characteristics of hard particles, such as E_p , V_p , and κ , irrespective of geometric size factor λ . As such, Fig. 8(b) presents that E_e maintains a stable quantity as λ exceeds its critical threshold. In addition, before getting to the threshold state, E_e decreases with the increase of λ . It appears that it is the first time to our knowledge that such a conclusion is present. More interestingly, in accordance with the definition of λ , the interfacial volume fraction and the effective elastic modulus intensively depend on the coupling of interfacial dimension and particle size, rather than the single factor. This finding provides an efficient tool that can allow researchers to control the geometric size factor to design particulate composites for their mechanical applications.

We also investigate the effect of particle size distribution (PSD) on the effective elastic modulus of particulate composites. To this end, we select three specific distribution functions: the power-law, Fuller, and equal volume fraction (EVF), which have been extensively used for spherical particle size distributions in the modeling studies of particulate materials [4,9,23], as given in the following formula.

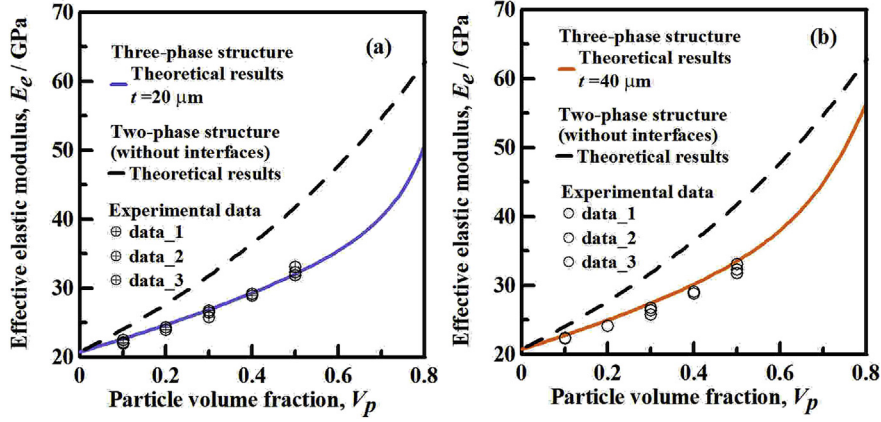


Fig. 6. Comparisons of the proposed three-phase theoretical framework with experimental data of the elastic modulus of particulate materials with two interfacial dimensions of (a) $t = 20 \mu\text{m}$ and (b) $t = 40 \mu\text{m}$ reported by Yang [31], and with the two-phase theoretical scheme without interface phase. Theoretical parameters follow Yang's experiment, in which the average size of particles is $450 \mu\text{m}$, $E_i = 0.2 E_m$ for $t = 20 \mu\text{m}$, and $E_i = 0.5 E_m$ for $t = 40 \mu\text{m}$. The average aspect ratio of particles of $\kappa = 2.021$.

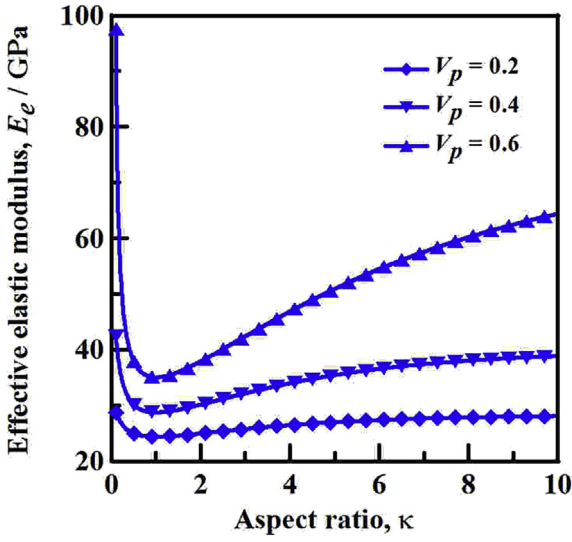


Fig. 7. The effective elastic modulus E_e versus the aspect ratio κ for three particle volume fractions of $V_p = 0.2, 0.4$, and 0.6 . The basic parameters are in agreement with those in Fig. 6(b).

$$f_N(R) = \begin{cases} \frac{-q}{2R^{q+1}(R_{\max}^{-q} - R_{\min}^{-q})} & \left\{ \begin{array}{l} q = 2.5 \rightarrow \text{Fuller} \\ q = 3.0 \rightarrow \text{EVF} \end{array} \right. \\ \frac{(b-1)R^{-b}}{R_{\min}^{1-b} - R_{\max}^{1-b}} & \text{where } b \neq 1 \rightarrow \text{power law} \end{cases} \quad (22)$$

where $f_N(R)$ is the number-based probability function of spherical particles, R_{\max} and R_{\min} are the maximum and minimum radii of spherical particles, respectively. b is an exponent with respect to the power-law distribution, the value of which is usually prescribed to more than unity. We transform a PSD of spherical particles into the PSD of anisotropic particles by the definition of equivalent diameter D_{eq} . By substituting D_{eq} into R mentioned in the above formula, the three PSDs for anisotropic particles are displayed by

$$f_N(D_{eq}) = \begin{cases} \frac{-q}{D_{eq}^{q+1}(D_{\max eq}^{-q} - D_{\min eq}^{-q})} & \left\{ \begin{array}{l} q = 2.5 \rightarrow \text{Fuller} \\ q = 3.0 \rightarrow \text{EVF} \end{array} \right. \\ \frac{b-1}{D_{\min eq}^{1-b} - D_{\max eq}^{1-b}} D_{eq}^{-b} & \text{where } b \neq 1 \rightarrow \text{power law} \end{cases} \quad (23)$$

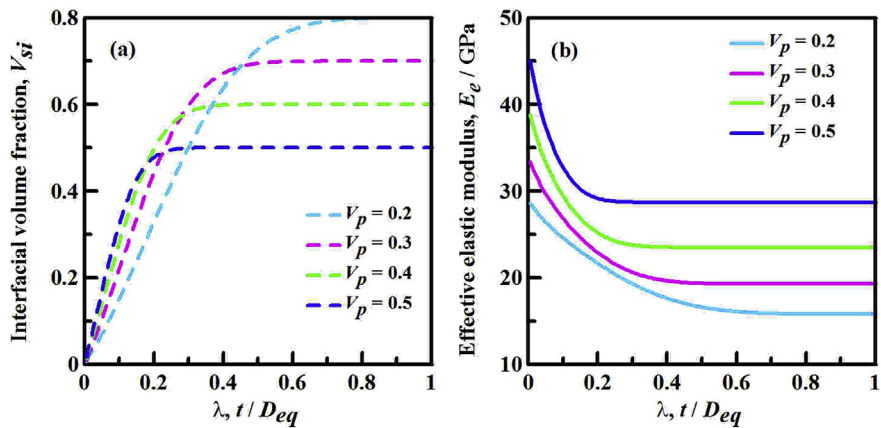


Fig. 8. (a) The interfacial volume fraction V_{si} versus the geometric size factor λ and (b) the effective elastic modulus E_e versus the geometric size factor λ for different particle volume fractions V_p . The basic parameters in Fig. 8 are in agreement with those in Fig. 6(b).

where $f_N(D_{eq})$ is the number-based probability function of anisotropic particle systems, D_{maxeq} and D_{mineq} are the maximum and minimum equivalent diameters of anisotropic particles. It is worth stressing that the above three particular distributions are just introductory examples for demonstrating the influence of PSD, other distribution functions can also be transformed in the theoretical and modeling researches of polydisperse particulate materials in a similar manner.

Fig. 9 presents the effective elastic modulus E_e versus particle volume fraction V_p for Fuller distribution, EVF distribution, and the power-law distributions with exponents of $b = 2.0, 3.0$, and 5.0 . From Figs. 3, 5–9, we find that E_e increases in a manner that is proportional to V_p , regardless of monodisperse or polydisperse particle systems, except the lead case presented in Fig. 5. It is in fact that, as a reinforcement phase, the larger volume fraction of hard particles generates the greater elastic modulus of particulate composites. This agrees with the conclusions reported in the literature. For the lead case presented in Fig. 5, the lead particles are not treated as a reinforcement phase in materials, but as a weak phase, since the elastic modulus of lead particles is lower than that of a matrix.

On the other hand, for a given V_p , Fig. 9 shows that E_e falls in the order power-law distribution of $b = 2.0 >$ power-law distribution of $b = 3.0 >$ Fuller distribution $>$ EVF distribution $>$ power-law distribution of $b = 5.0$. Interestingly, according to Eq. (23), we find that Fuller and EVF distributions essentially belong to the power-law distributions corresponding to $b = 3.5$ and 4.0 . In other words, Fig. 9 eventually presents that the effective elastic modulus decreases with the increase of exponent of power-law distribution. It is an interesting generalization that can guide for the design of particulate materials by selecting a suitable exponent of power-law distribution to control their elastic properties. As a matter of fact, under the same particle volume fraction, the larger exponent of power-law distribution generates the more fine particles and therefore has a larger surface area of solid phase, which leads to a more amount of interfaces with weak stiffness [23]. As an introductory example, Fig. S4 (see S5) visualizes two two-phase composite structures possessing the same particle volume fraction with the power-law distributions of $b = 2.0$ and 5.0 . It can be seen that

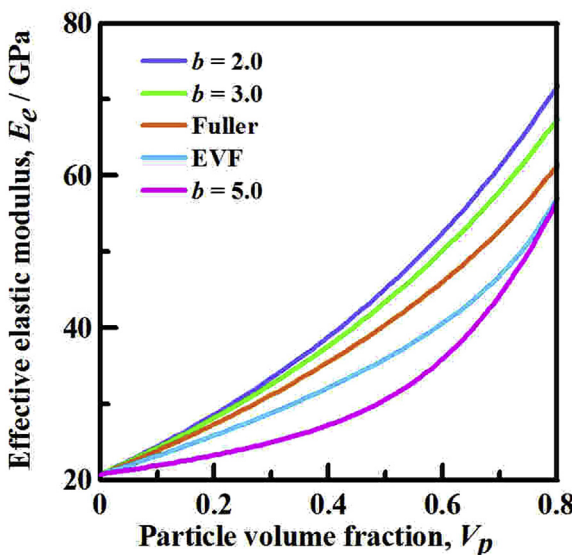


Fig. 9. The effective elastic modulus E_e versus particle volume fraction V_p for Fuller distribution, EVF distribution, and the power-law distributions with exponents of $b = 2.0, 3.0$, and 5.0 . The maximum and minimum equivalent diameters of $D_{maxeq} = 16$ and $D_{mineq} = 0.15$.

the number of fine particles for the power-law distribution of $b = 5.0$ is obviously more than that for the power-law distribution of $b = 2.0$.

6. Conclusions and remarks

This paper proposed a theoretical framework in details to predict the effective elastic modulus of three-phase particulate composites consisting of mono-/polydisperse spheroidal particles, soft interfaces, and a homogeneous matrix. The theoretical framework quantitatively addressed how the interfacial properties such as the interfacial volume fraction, dimension, and elastic modulus affect the overall elastic modulus of particulate composites. By comparing with extensive experimental data, numerical results, and theoretical approximations reported in the literature, the present theoretical framework was demonstrated to be an efficient tool for the accurate estimation of effective elastic modulus of particulate composites. In addition, the present scheme was used to evaluate the effects of the interfacial properties and spheroidal particle geometries on the effective elastic modulus. It was revealed that the effective elastic modulus increases with the increase of the interfacial elastic modulus. Also, the effect of aspect ratio of spheroidal particles on the effective elastic modulus has an intrinsic similarity to that on the interfacial volume fraction, to be specific, the anisotropy of particles leads to the higher effective elastic modulus and higher interfacial volume fraction. This theoretical generalization confirmed that the packing density of ellipsoids sharply increases as anisotropic particles deviate slightly from perfect spheres, which has been studied by computer simulations in the literature. A quantitative manner was proposed for the first time that the effective elastic modulus closely relates to the threshold of geometric size factor. Moreover, the theoretical results further demonstrated that the effective elastic modulus decreases with the increase of exponents of the power-law distribution of particle sizes. The proposed theoretical framework and these interesting observations provide us with significant insights on optimizing the microstructural physical characteristics for the design of particulate composites.

On the other hand, from Fig. 8(a), it has been clearly shown that, as the geometric size factor increases, soft interfacial layers gradually enlarge and even potentially occupy to the more matrix material. Thus, interfaces may generate a percolating path within material structures. It is not merely of structural significance but also results in dramatic changes of mechanical properties of materials near the percolation threshold. Accordingly, in future works, we will study the percolation behaviors of soft interfaces in more details, and discuss how the physical properties are affected on the percolation threshold.

Acknowledgments

The authors acknowledge financial supports from National Natural Science Foundation Project of China (Grant No. 11402076), Natural Science Foundation Project for Jiangsu Province (Grant No. BK20130841), China Postdoctoral Science Foundation Funded Project (Grant Nos. 2014M560385 and 2015T80493), the Open Research Fund of State Key Laboratory of Structural Analysis for Industrial Equipment (Grant No. GZ1405), the Open Research Fund of State Key Laboratory of Simulation and Regulation of Water Cycle in River Basin (Grant No. IWHR-SKL-201511), the Open Research Fund of Jiangsu Key Laboratory of Construction Materials (Grant No. CM2014-03), Jiangsu Postdoctoral Science Foundation Project (Grant No. 1402053C), and Research Special of the China Institute of Water Resources and Hydropower Research (Grant No. KY1640).

Appendix A. Supplementary data

Supplementary data related to this article can be found at <http://dx.doi.org/10.1016/j.compscitech.2016.04.011>.

References

- [1] X.Q. Fang, X.L. Liu, M.J. Huang, J.X. Liu, Dynamic effective shear modulus of nanocomposites containing randomly distributed elliptical nano-fibers with interface effect, *Compos. Sci. Technol.* 87 (2013) 64–68.
- [2] Y. Shen, Y.H. Lin, C.W. Nan, Interfacial effect on dielectric properties of polymer nanocomposites filled with core/shell-structured particles, *Adv. Funct. Mater.* 17 (2007) 2405–2410.
- [3] S. Alexander, R. Xiao, T.D. Nguyen, Modeling the thermoviscoelastic properties and recovery behavior of shape memory polymer composites, *J. Appl. Mech.* 81 (2014) 041003.
- [4] W.X. Xu, H.S. Chen, W. Chen, L.H. Jiang, Prediction of transport behaviors of particulate composites considering microstructure of soft interfacial layers around ellipsoidal aggregate particles, *Soft Matter* 10 (2014) 627–638.
- [5] S. Torquato, *Random Heterogeneous Materials: Microstructure and Macroscopic Properties*, Springer-Verlag, New York, 2002.
- [6] Z. Wang, X.Y. Jin, W.Q. Chen, Ch Zhang, C.Q. Fu, H.Y. Gong, Micro-scaled size-dependence of the effective properties of 0-3 PZT-cement composites: experiments and modeling, *Compos. Sci. Technol.* 105 (2014) 183–189.
- [7] H.L. Duan, X. Yi, Z.P. Huang, J. Wang, A unified scheme for prediction of effective moduli of multiphase composites with interface effects. part I: theoretical framework, *Mech. Mater.* 39 (2007) 81–93.
- [8] K.L. Scrivener, A.K. Crumbie, P. Laugesen, The interfacial transition zone (ITZ) between cement paste and aggregate in concrete, *Interf. Sci.* 12 (2004) 411–421.
- [9] H.Y. Ma, Z.J. Li, Multi-aggregate approach for modeling interfacial transition zone in concrete, *ACI Mater. J.* 111 (2014) 189–200.
- [10] Y. Xie, D.J. Corr, F. Jin, H. Zhou, S.P. Shah, Experimental study of the interfacial transition zone (ITZ) of model rock-filled concrete (RFC), *Cem. Concr. Comp.* 55 (2015) 223–231.
- [11] R.M. Christensen, K.H. Lo, Solutions for effective shear properties in three phase sphere and cylinder models, *J. Mech. Phys. Solids* 27 (1979) 315–330.
- [12] R. Hill, A self-consistent mechanics of composite materials, *J. Mech. Phys. Solids* 13 (1965) 213–222.
- [13] Z. Hashin, S. Shtrikman, A variational approach to the theory of the effective magnetic permeability of multiphase materials, *J. Appl. Phys.* 33 (1962) 3125–3131.
- [14] Z. Hashin, Thermoelastic properties of particulate composites with imperfect interface, *J. Mech. Phys. Solids* 39 (1991) 745–762.
- [15] T. Mori, K. Tanaka, Average stress in matrix and average elastic energy of materials with misfitting inclusions, *Acta Metall.* 21 (1973) 571–574.
- [16] A.N. Norris, A.J. Callegari, P. Sheng, A generalized differential effective medium theory, *J. Mech. Phys. Solids* 33 (1985) 525–543.
- [17] Y. Benveniste, Exact results for the local fields and the effective moduli of fibrous composites with thickly coated fibers, *J. Mech. Phys. Solids* 71 (2014) 219–238.
- [18] S. Torquato, Effective stiffness tensor of composite media: I. exact series expansions, *J. Mech. Phys. Solids* 45 (1997) 1421–1448.
- [19] S.Y. Fu, X.Q. Feng, B. Lauke, Y.W. Mai, Effects of particle size, particle/matrix interface adhesion and particle loading on mechanical properties of particulate-polymer composites, *Compos. Part B* 39 (2008) 933–961.
- [20] M. Wang, N. Pan, Predictions of effective physical properties of complex multiphase materials, *Mater. Sci. Eng. R.* 63 (2008) 1–30.
- [21] E.J. Garboczi, D.P. Bentz, Multiscale analytical/numerical theory of the diffusivity of concrete, *Adv. Cem. Based Mater.* 8 (1998) 77–88.
- [22] W.X. Xu, H.S. Chen, Analytical and modeling investigations of volume fraction of interfacial layers around ellipsoidal aggregate particles in multiphase materials, *Model. Simul. Mater. Sci. Eng.* 21 (2013) 015005.
- [23] W.X. Xu, W. Chen, H.S. Chen, Modeling of soft interfacial volume fraction in composite materials with complex convex particles, *J. Chem. Phys.* 140 (2014) 34704.
- [24] W.X. Xu, H.S. Chen, Q.L. Duan, W. Chen, Strategy for interfacial overlapping degree in multiphase materials with complex convex particles, *Powder Technol.* 283 (2015) 455–461.
- [25] J.R. Wills, Bounds and self-consistent estimates for the overall moduli of anisotropic composites, *J. Mech. Phys. Solids* 25 (1977) 185–202.
- [26] P.P. Castañeda, J.R. Willis, The effect of spatial distribution on the effective behavior of composite materials and cracked media, *J. Mech. Phys. Solids* 43 (1995) 1919–1951.
- [27] H.L. Duan, B.L. Karighaloo, J. Wang, X. Yi, Effective conductivities of heterogeneous media containing multiple inclusions with various spatial distributions, *Phys. Rev. B* 73 (2006) 174203.
- [28] B.L. Lu, S. Torquato, Nearest-surface distribution functions for polydisperse particle systems, *Phys. Rev. A* 45 (1992) 5530–5544.
- [29] D.S. McLachlan, M.B. Blazkiewicz, R.E. Newnham, Electrical resistivity of composites, *J. Am. Ceram. Soc.* 73 (1990) 2187–2203.
- [30] A.F. Stock, D.J. Hannant, R.I.T. Williams, The effect of aggregate concentration upon the strength and modulus of elasticity of concrete, *Mag. Concr. Res.* 31 (1979) 225–234.
- [31] C.C. Yang, Effect of the transition zone on the elastic moduli of mortar, *Cem. Concr. Res.* 28 (1998) 727–736.
- [32] A. Donev, I. Cisse, D. Sachs, E.A. Variano, F.H. Stillinger, R. Connelly, S. Torquato, P.M. Chaikin, Improving the density of jammed disordered packings using ellipsoids, *Science* 303 (2004) 990–993.
- [33] Z.Y. Zhou, R.P. Zou, D. Pinson, A.B. Yu, Dynamic simulation of the packing of ellipsoidal particles, *Ind. Eng. Chem. Res.* 50 (2011) 9787–9798.
- [34] A. Baule, R. Mari, L. Bo, L. Portal, H.A. Makse, Mean-field theory of random close packings of axisymmetric particles, *Nat. Commun.* 4 (2013) 2194.
- [35] G. Ramesh, E.D. Sotellino, W.F. Chen, Effect of transition zone on elastic moduli of concrete materials, *Cem. Concr. Res.* 26 (1996) 611–622.
- [36] L.B. Wang, X.R. Wang, L. Mohammad, C. Abadie, Unified method to quantify aggregate shape angularity and texture using Fourier analysis, *ASCE J. Mater. Civ. Eng.* 17 (2005) 498–504.